

Numerical Simulation of Coupled CFD-flight Mechanics and Taguchi's Approach for Reliability and Safety Assessments in the Hot Stage Separation of a Launch Vehicle

D. Nasiri ¹, M. Adami ^{1†}, H. Taei ² and H. Parhizkar ³

¹ Faculty of Mechanical Engineering, Malek-ashtar University of Technology, Isfahan, Iran

² Faculty of Engineering, Department of Aerospace Engineering, University of Isfahan, Isfahan, Iran

³ Department of Mechanical Engineering, Malek-ashtar University of Technology, Tehran, Iran

†Corresponding Author Email: adami@mut-es.ac.ir

ABSTRACT

This research presents a numerical simulation of a two-stage launch vehicle's hot stage separation process. Important parameters, such as the separation altitude, flight Mach number, and the angle of attack during separation, were investigated. The effects of these factors and the motor thrust parameter on the distance between the two stages post-separation were evaluated using the Taguchi method. Numerical analysis was performed using ANSYS Fluent, solving the three-dimensional flow field under the six degrees of freedom (6DOF) assumption. The SST $k-\omega$ turbulence model was employed for turbulence modeling, with a tetrahedral unstructured mesh used for the computational domain. The simulation results showed that increasing the separation altitude from 10 km to 20 km increased the distance between the two stages by 5.75%, primarily due to reduced air density and drag forces. Raising the flight Mach number from 2 to 3.2 increased the separation distance of two stages by 2.2%. Additionally, a higher angle of attack increased the deviation of the stages from their original trajectory, necessitating stage control after separation. Among the parameters studied, the motor thrust has the most significant effect on increasing the distance between the stages and preventing collisions. In contrast, the angle of attack has the most minor influence.

Article History

Received October 19, 2024

Revised March 4, 2025

Accepted April 1, 2025

Available online June 3, 2025

Keywords:

Two-stage launch vehicle

Taguchi's approach

Altitude

Flight Mach number

Angle of attack

1. INTRODUCTION

In the aerospace industry, launch vehicles are used to reach high altitudes and deliver payloads into space. These vehicles can be single-stage or multistage. In a multistage configuration, the vehicle consists of two or more stages that separate during flight. Multistage configurations offer advantages over single-stage vehicles, including reduced fuel requirements, increased final payload velocity, and greater payload capacity, ultimately lowering costs. However, the complexity of the separation process reduced flight reliability, and increased construction costs are significant disadvantages of multistage vehicles.

Figure 1 illustrates a schematic of a two-stage launch vehicle with a payload. The two stages are connected by an inter-stage adapter, which typically resembles a lattice truss. The hot exhaust gas from the second stage motor is discharged through holes integrated into this adapter. In this study, it was not investigated due to the complexity of modeling the inter-stage adapter.

The stage separation process is categorized into cold and hot separation based on the motor ignition timing for each stage. In cold separation, the second stage motor is ignited only after the stages have fully separated.

In hot separation, as shown in Fig. 2, the second stage motor is ignited before the stages separate. At time t_1 , the motor in stage two ignites while the motor in stage one has started to shut down. The separation mechanism then operates, breaking the connection between the stages.

The exhaust gases from stage two, at time t_3 , push the stages apart (Goldman, 1969).

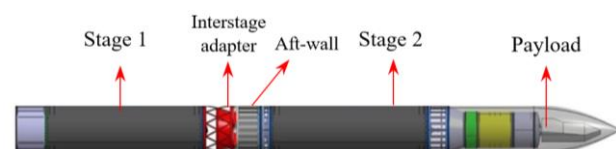


Fig. 1 Schematic of a two-stage launch vehicle

Nomenclature	
F	net force on body
I_{xx}	inertia moment at yaw plane
I_{yy}	inertia moment at roll plane
I_{zz}	inertia moment at pitch plane
I_{xy}	product inertia moment at yaw plane
I_{xz}	product inertia moment at roll plane
I_{yz}	product inertia moment at pitch plane
L	angular momentum vector
M	moment vector
Ma	Mach number
p	angular velocity component of x-axis
q	angular velocity component of y-axis
r	angular velocity component of z-axis
u	velocity component at x-axis direction
v	velocity component at y-axis
w	velocity component at z-axis
ω	angular velocity

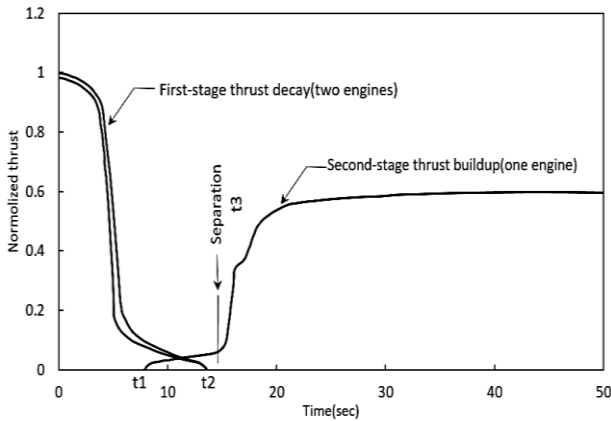


Fig. 2 Process of hot separation of a two-stage launch vehicle (Goldman, 1969)

In hot separation, the timing of the second stage motor ignition is important. If the motor ignites too early, excessive heat from the exhaust gases can cause damage to the structure of both stages. This is particularly hazardous if the stages use liquid-fueled motors with poor thermal insulation, potentially leading to an explosion (Mitikov & Shynkarenko, 2023).

Research into hot separation dates back to the 1960s. Wasko (1961) conducted wind tunnel tests to study the pressure distribution, aerodynamic forces, and their effects on stage stability during separation. Since the 1990s, numerical methods have become more prevalent over experimental methods, due to their cost-effectiveness, faster results, and ability to test a wide range of parameters without physical constraints. Numerical simulations can provide detailed data that might be difficult or dangerous to measure in physical experiments, and it is easier to modify parameters and test different conditions in a numerical simulation for a more comprehensive analysis of various factors affecting the separation process.

Wang et al. (2009) and Huseman (1995) numerically simulated the hot separation of the Titan IV rocket's first stage using the Euler equation. Their calculated pressure distribution matched well with experimental results. Wang (1997) further numerically solved the coupled CFD and rigid dynamic equations for hot separation using the finite volume method, obtaining the flow distribution in the intermediate region between the two stages. During stage separation, the gap between the stages can be considered as a hole allows the motor exhaust gases to enter the supersonic airflow, using this simplification, one can use the research results in this area to predict hot stage

separation flow conditions (Lawson & Barakos, 2011). Kumar et al. (1998) developed an analytical model to calculate forces and moments on the cylindrical fairing of an active stage motor (stage two), achieving good agreement with experimental and numerical data. Roshanian and Talebi (2008) analytically studied cold and hot separation, deriving dynamic equations to govern stage motion and assess separation forces in a vacuum environment. Monte Carlo method is utilized to investigate parameter uncertainties in their study. In a study by Li et al. (2014), the shape of the first-stage nose, which interacts with the hot exhaust gas from the second stage motor, was numerically investigated using three different configurations: flat, spherical, and conical, analyzed in two dimensions. The results demonstrated that the spherical nose configuration reduced the power transfer from the hot exhaust gas of the second stage motor by 45% compared to the flat configuration, consequently decreasing the separation speed of the two stages. Similarly, the conical configuration reduced the power transfer by 46% relative to the flat configuration, further highlighting the influence of nose geometry on aerodynamic performance during stage separation.

Li et al. (2016) analyzed hot separation for a two-stage launch vehicle with solid-fueled motors, finding that a non-zero angle of attack during separation increased angular changes in the second stage, negatively impacting trajectory. To minimize these effects, the angle of attack should be as close to zero as possible during separation.

In engineering design, uncertainty in design parameters is inevitable. One of the simplest methods for studying uncertainty is the Monte Carlo method, widely used in fluid dynamics for rarefied atmospheric flow and boundary layer growth (Bird, 1981; Oran et al., 1998). Bird (1978) applied this method to engineering problems like rarefied gas flow analysis, while Collins & Knox (1994) used it for supersonic boundary layer flow analysis. Although effective, the Monte Carlo method requires extensive computational time and cost, especially with software like ANSYS Fluent. To address this, the Taguchi method offers an optimized statistical model for investigating the effects of design parameters while significantly reducing the number of required simulations, thereby lowering both time and costs. Rao et al. (2006) studied parameters affecting cold separation and compared uncertainty results from the Monte Carlo, worst-case, and multivariable methods for variables such as relative stage velocity and angular rates. Singaravelu et al. (2009) also calculated uncertainties using these

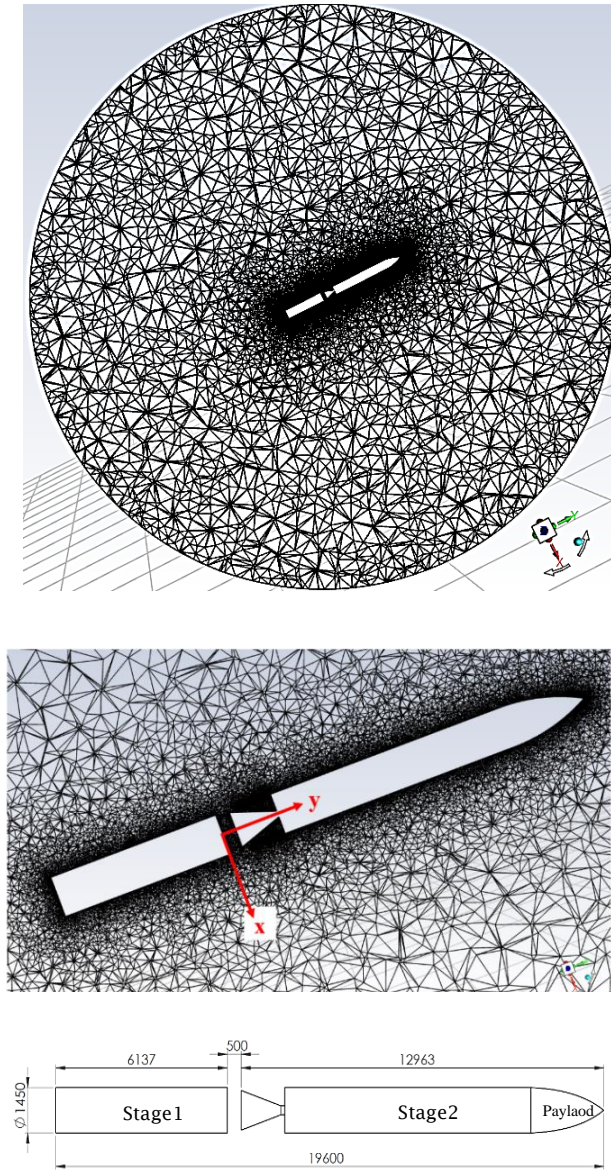


Fig. 3 Computational mesh and dimensions (in mm-[Martins, 2020](#)) of the launch vehicle used in this study

methods and found that the Taguchi method required fewer simulations with comparable accuracy to the Monte Carlo method. [Simplicio and Bennani \(2015\)](#) investigated the uncertainty of separation dynamic factors using the worst-case method, applying the results to the VEGA launch vehicle. [Huitong et al. \(2015\)](#) modeled the dynamic behavior of a two-stage rocket during separation, determining the level of uncertainty in dynamic parameters using the Monte Carlo method.

This study aims to numerically investigate the hot separation of a two-stage launch vehicle, focusing on the effects of altitude, flight Mach number, and angle of attack and their associated uncertainties during separation. These parameters have not been thoroughly studied in the existing literature.

2. PROBLEM DESCRIPTION

In this research, the three-dimensional hot separation process of a two-stage launch vehicle during the separation of the first and second stages is studied. The geometry and overall dimensions of the launch vehicle are shown in Fig. 3. The vehicle consists of two similar stages and a payload, and the vehicle's dimensions are based on the VLM-1 manufactured in Brazil ([Martins, 2020](#)).

The computational domain is meshed, as shown in Fig. 3, with the launch vehicle inclined at a 30-degree angle to the local horizontal at the time of separation. A tetrahedral unstructured mesh is used, and the ANSYS Fluent solver is employed to simultaneously solve the six degrees of freedom (6DOF) flight dynamics and aerodynamic equations for the separation process. The launch vehicle is treated as a 3D body with 6DOF motion.

The general equation of motion for six degrees of freedom(6DOF) is as follows ([Roshanian & Talebi, 2008](#)):

$$m \frac{dV}{dt} + m\omega \times V = F_t \quad (1)$$

Where in Eq. (1), the values of V , ω , and F_t which are the vectors of linear velocity, angular velocity and force, respectively, are defined as follows:

$$V = u i + v j + w k$$

$$\omega = pi + qj + rk \quad (2)$$

$$F_t = F_x i + F_y j + F_z k$$

The values of p , q , and r are the angular velocity components around the coordinate axes of the inertial XYZ system.

The translational motion equation can be derived from Eq. (1) and Eq. (2) as follows:

$$\begin{cases} m(\dot{u} + qw - rv) = F_x \\ m(\dot{v} + ru - pw) = F_y \\ m(\dot{w} + pv - qu) = F_z \end{cases} \quad (3)$$

The angular motion of a rigid body is described by Eq. (4):

$$\frac{dL}{dt} + \omega \times L = M \quad (4)$$

L is the angular momentum vector, and M is the external moment vector.

$$M = M_x i + M_y j + M_z k \quad (5)$$

The angular momentum vector L is expressed as:

$$\begin{bmatrix} L_x \\ L_y \\ L_z \end{bmatrix} = \begin{bmatrix} I_{xx} & -I_{xy} & -I_{xz} \\ -I_{xy} & I_{yy} & -I_{yz} \\ -I_{xz} & -I_{yz} & I_{zz} \end{bmatrix} \begin{bmatrix} p \\ q \\ r \end{bmatrix} \quad (6)$$

Substituting Eq. (5) and Eq. (6) into Eq. (4) yields:

$$\begin{cases} I_{xx}\dot{p} - I_{xy}\dot{q} - I_{xz}\dot{r} + q(-pI_{xz} - qI_{yz} + rI_{zz}) \\ \quad - r(-pI_{xy} + qI_{yy} - rI_{yz}) = M_x \\ -I_{xy}\dot{p} + I_{yy}\dot{q} - I_{yz}\dot{r} - p(-pI_{xz} - qI_{yz} + rI_{zz}) \\ \quad + r(pI_{xx} - qI_{xy} - rI_{xz}) = M_y \\ -I_{xz}\dot{p} - I_{yz}\dot{q} + I_{zz}\dot{r} + p(-pI_{xy} + qI_{yy} - rI_{yz}) \\ \quad - q(pI_{xx} - qI_{xy} - rI_{xz}) = M_z \end{cases} \quad (7)$$

Table 1 Motor specifications for the two stages of the launch vehicle

Fuel Type	Solid
Thrust (kN)	400(90,000 lbf)
Rate of Burn(kg/s)	135.3
Lift off weight stage1 (kg)	12900
Propellant weight stage1 (kg)	11500
Lift off weight stage 2 (kg)	14104
Propellant weight stage 2 (kg)	11500

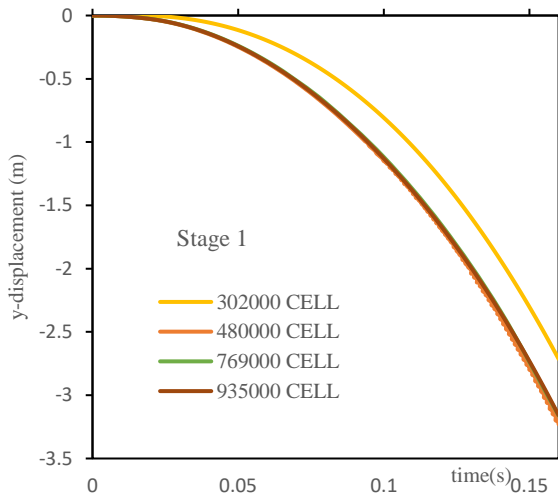


Fig. 4 Mesh independence study

In Eq. (7), F_x , F_y , F_z , M_x , M_y and M_z represent the external forces and moments acting on the body. These forces and moments are all created due to external forces acting on the body such as aerodynamic forces, thrust forces, gravitational forces, etc.

In this study, the launch vehicle has a mass of 27 tons and consists of two stages, both powered by solid fuel motors. Solid fuel motors are chosen due to their lower cost and reduced construction complexity (Matsuo & Kawaguchi, 1995). The motor specifications for the two stages are presented in Table 1.

The following assumptions are made for the simulation:

1-Due to the short duration of the hot separation process, the fuel mass in the second stage motor is assumed to remain constant, and the center of mass of the assembly does not change.

2- Changes in gravity and Earth's rotation are negligible over the short separation period.

3. MESH STUDY AND MODEL VALIDATION

In Fig. 4, corresponding to flight conditions of Mach 2.6, an altitude of 15.8 km, and a zero-degree angle of attack, four meshes with different cell counts were evaluated. The y-displacement of the first stage was compared over the 0 to 0.16-second interval after the start of separation process. The mesh with 480,000 cells provided results in good agreement with finer meshes and

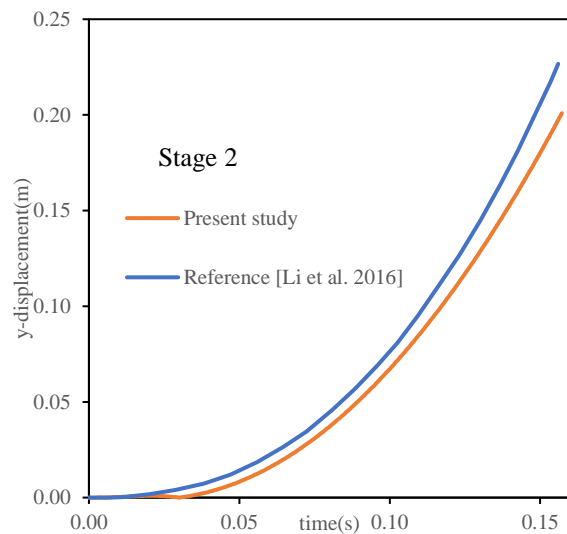
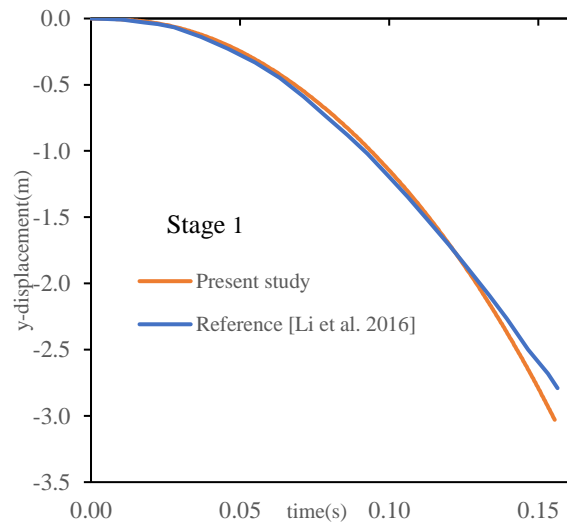


Fig. 5 Comparison y-displacement between present study and reference (Li et al., 2016)

was used for the simulations in this study due to its acceptable accuracy and computational efficiency.

The separation coordinate system(xyz) moves with a constant velocity equal to the launch vehicle's velocity at the time of separation. Displacement values for both stages are calculated relative to this coordinate system, with the y-axis aligned with the vehicle's longitudinal axis and the x and z axes perpendicular to it (Fig. 3).

For data validation, the results of this study were compared with those of Li et al. (2016) for a separation at 15.8 km altitude and Mach 2.6 with a zero-degree angle of attack. As shown in Fig. 5, after 0.16 seconds, the y-displacement of the first and second stages agrees well with the reference data (Li et al., 2016).

4. RESULTS AND DISCUSSION

4.1 Effect of Altitude

This study investigates the effect of separation altitude on the displacement of each stage during hot separation. The changes in y-displacement of each stage at altitudes

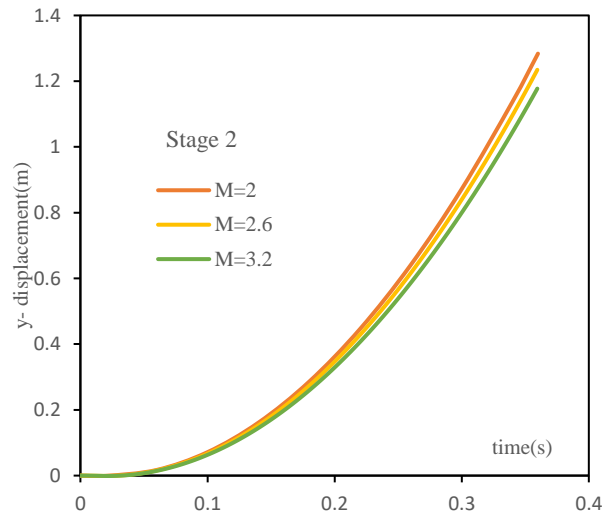
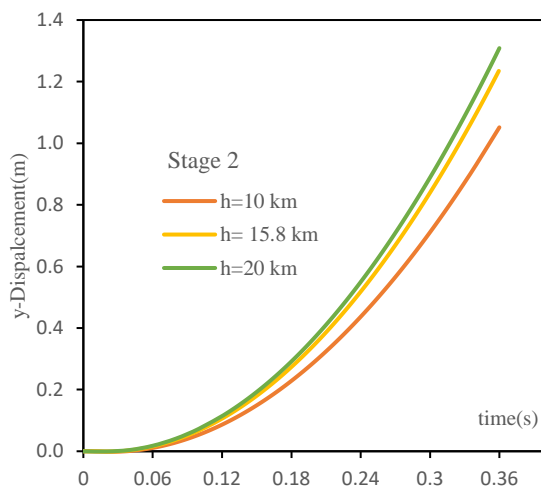
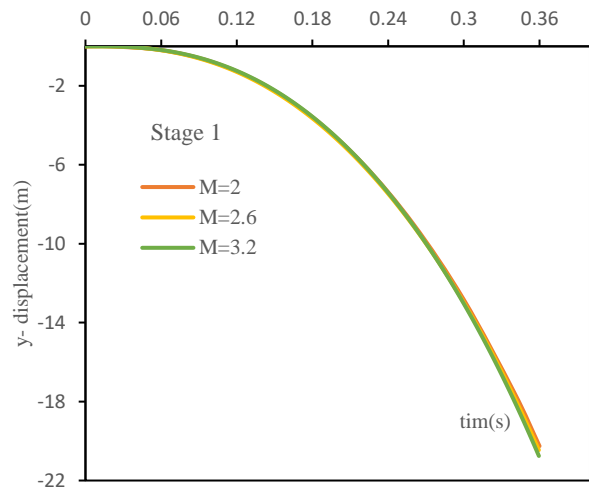
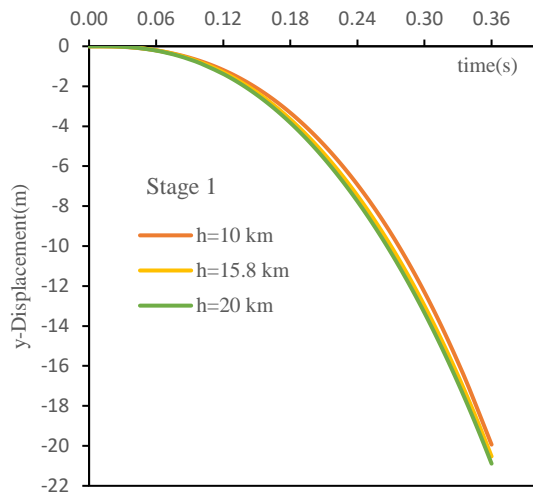


Fig. 6 Displacement in the y-direction of two stages at altitudes of 10, 15.8 and 20 km

Fig. 7 Displacement in the y-direction of two stages at Mach 2, 2.6 and 3.2

of 10 km, 15.8 km, and 20 km are shown in Fig. 6. The results indicate that increasing the altitude from 10 km to 20 km leads to a 5.75% increase in the distance between the two stages. In other words, the higher the altitude, the greater the distance between the two stages. This can be attributed to the decrease in air density with increasing altitude, which reduces the drag force acting on the stages after separation, allowing both stages to travel further in the direction of their movement.

4.2 Effect of Flight Mach

The impact of the flight Mach number at the moment of hot separation has been analyzed for Mach numbers 2, 2.6, and 3.2, as shown in Fig. 7. The flight altitude is 15 km, and the angle of attack is set to 0 degrees during separation.

As shown in Fig. 7, the y-displacement of the first stage increases with increasing Mach number, while the displacement of the second stage decreases. Overall, the distance between the two stages increases with higher Mach numbers. According to Fig. 7, increasing the flight Mach number from 2 to 3.2 results in a 2.2% increase in the distance between the stages. The drag force acting on

both stages increases with Mach number. For the first stage, this increased drag results in more significant displacement, while the second stage, experiencing both thrust and drag forces, moves less forward as the balance between these forces reduces its net forward motion.

Figure 8 shows the Mach contours around both stages at 0.32 seconds after the start of the separation process. In all cases, since the Mach number is greater than 1, shock waves are observed around both stages.

4.3 Effect of Angle of Attack

While a zero angle of attack is desirable during separation to prevent control issues and disturbances caused by asymmetric flow and forces, achieving this in practice is challenging due to uncertainties at the moment of separation. Therefore, the effect of varying angles of attack on stage separation is examined.

Figure 9 presents the y-displacement of the stages for Mach 2.6, altitude 15.8 km, and angles of attack of 0, 2, and 4 degrees. Changes in the angle of attack from 0 to 4 degrees have a minimal effect on the y-displacement of both stages. However, as seen in Fig. 10, the x-

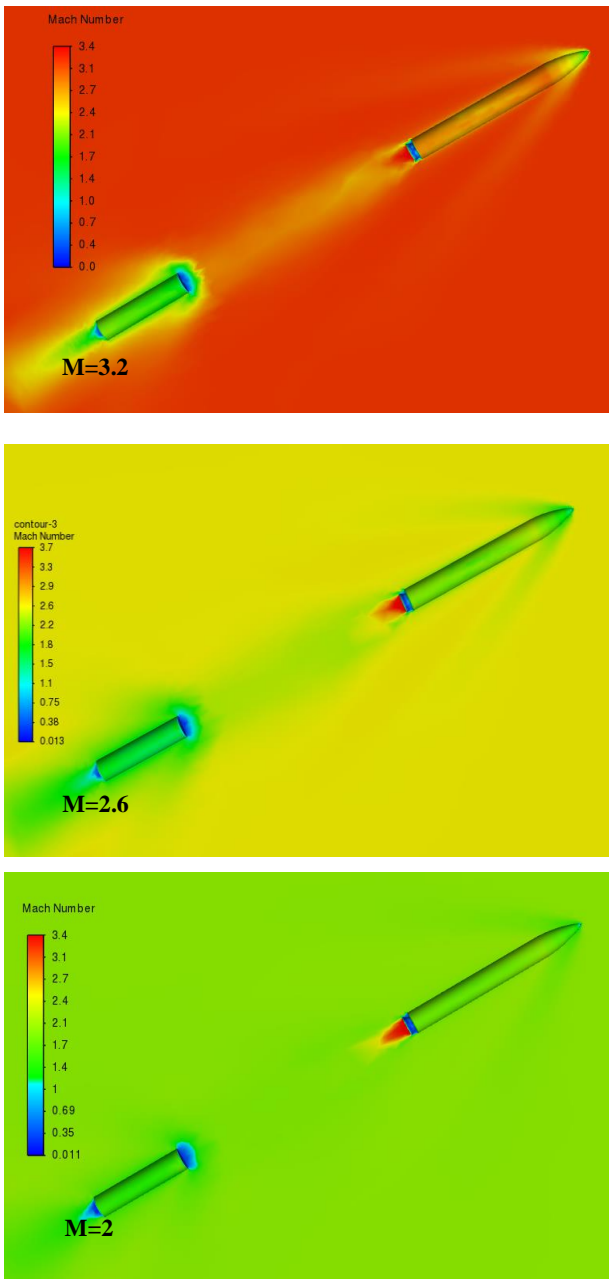


Fig. 8 Mach contours around the two stages at 0.32 seconds after separation for Mach 2, 2.6 and 3.2

displacement of the stages increases with the angle of attack. This deviation towards the negative x-axis occurs due to the angle of attack introducing a force component perpendicular to the launch vehicle's axis, causing a slight deviation from its path.

Figures 11 and 12 show the Mach contours for different angles of attack at 0.12 and 0.32 seconds after separation, respectively.

Figure 11 shows that the exit supersonic jet impacts the front surface of the first stage, leading to the formation of a bow shock. The flow resulting from this interaction is currently insufficient to pose significant challenges to the second stage nozzle. However, the combined effect of the exit supersonic jet and the free supersonic flow generates an expanded bow shock, which extends to the nozzle and

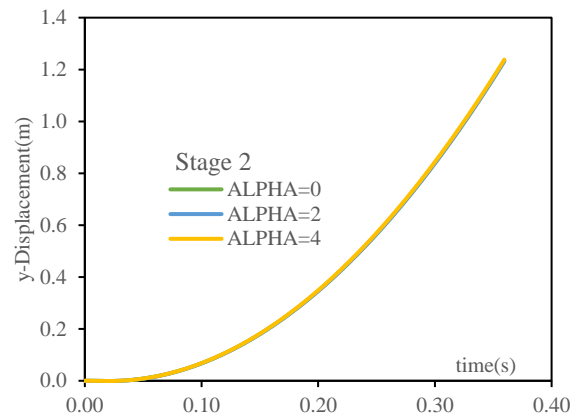
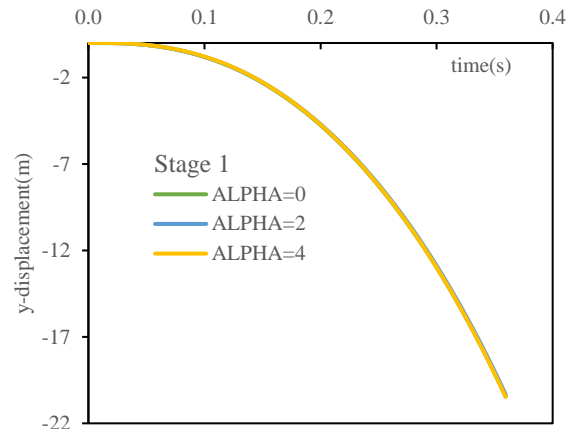


Fig. 9 Displacement in the y-direction of two stages at angles of attack $\alpha = 0, 2$ and 4 degree

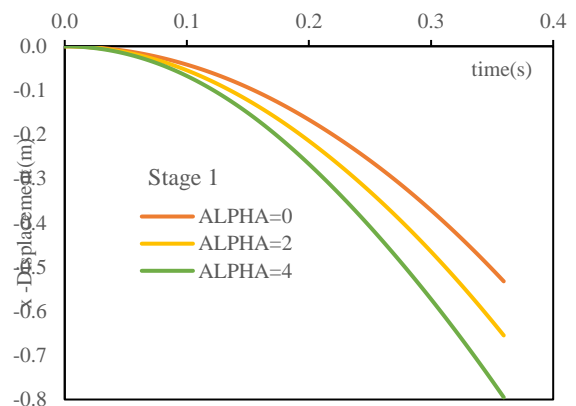
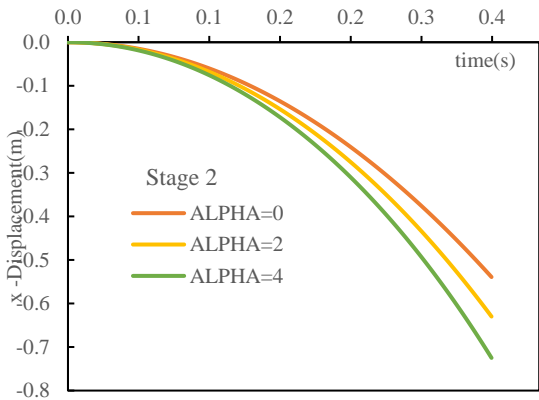


Fig. 10 Displacement in the x-direction of two stages at angles of attack $\alpha=0, 2$ and 4 degree

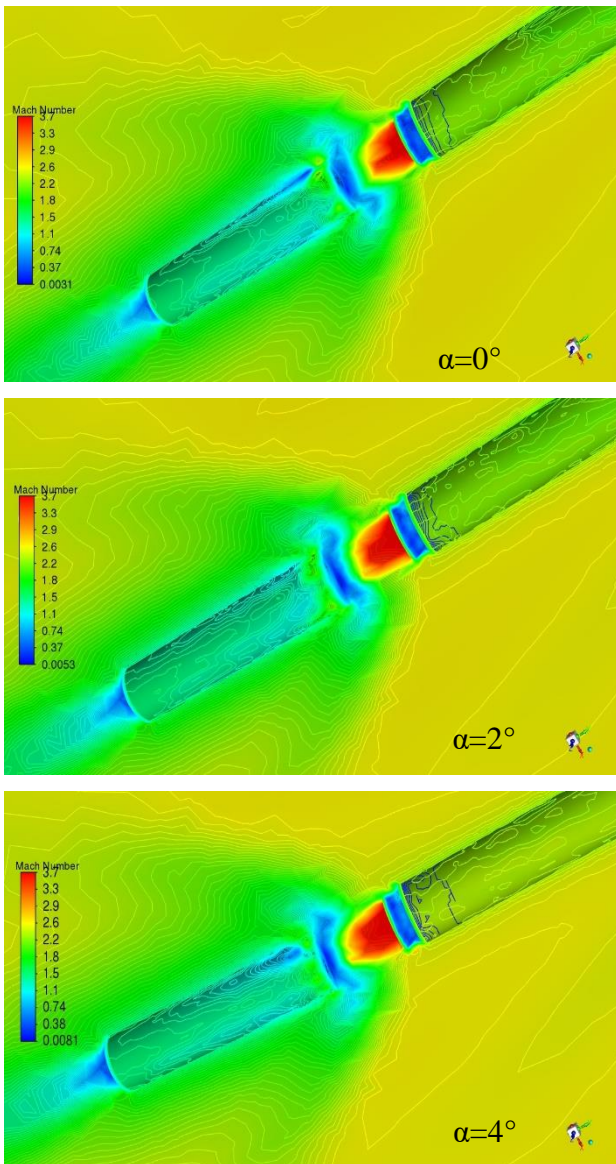


Fig. 11 Mach contours at different angles of attack at 0.12 seconds after separation

aft-wall of the second stage. Further research is required to investigate the shock's interaction with the boundary layer, boundary layer separation on the aft-wall and the associated heating effects in greater detail. Additionally, as the angle of attack increases, the bow shock shifts closer to the windward side of the first stage and farther from its aft side. Nevertheless, these positional changes have minimal impact on the overall findings of the current analysis.

Figure 12 also indicates as the angle of attack increases, the flow distribution around the stages becomes more asymmetric, complicating their motion and requiring careful control.

5. TAGUCHI METHOD

In many processes, numerous parameters affect the final output, necessitating the design of experiments (DOE) to identify the impact of these parameters and their

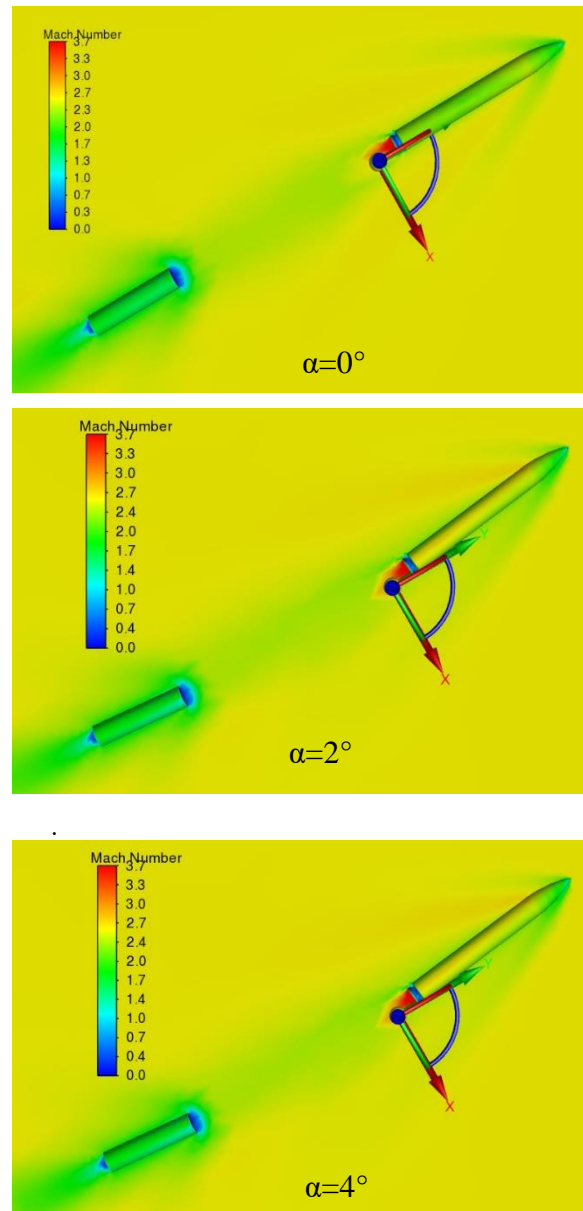


Fig. 12 Mach contours at different angles of attack at 0.32 seconds after separation

interactions. The Taguchi method provides an efficient optimization technique using orthogonal arrays, which reduces the number of required experiments while maximizing the information obtained. This allows all parameters' effects and interactions to be assessed with fewer experiments or simulations.

In the Taguchi method, the first step is to select the influential factors (parameters) and the levels of variation for each factor. Based on the number of factors and levels, the number of experiments is determined using orthogonal arrays. In this study, the effects of motor thrust, separation altitude, flight Mach number, and angle of attack on the y-displacement the two stages were examined, with three levels of variation for each factor, as shown in Table 2

Based on the four factors with three levels of variation in the Table 2, the Taguchi method suggests the experimental design shown in Table 3.

Table 2 Input factors (parameters) and their levels in the Taguchi method for hot separation

Factors	Levels (at the separation moment)		
	Level 1	Level 2	Level 3
Altitude (km)	14	15	16
Angle of attack (degree)	-1	0	1
Flight Mach number	2.3	2.6	2.9
Motor thrust (kN)	380	400	420

Table 3 Taguchi method’s experimental design for hot separation

Row	Altitude (km)	Angle of attack (degree)	Flight Mach number	Motor thrust (kN)
1	14	-1	2.3	380
2	15	0	2.6	380
3	16	1	2.9	380
4	16	0	2.3	400
5	14	1	2.6	400
6	15	-1	2.9	400
7	15	1	2.3	420
8	16	-1	2.6	420
9	14	0	2.9	420

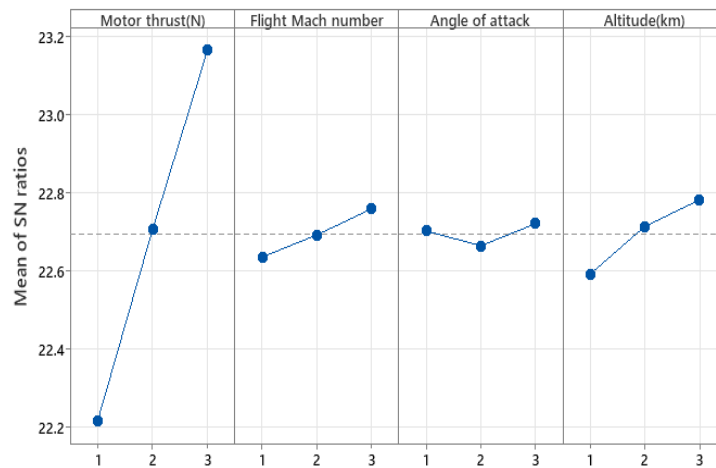


Fig. 13 S/N ratio plots for influential parameters in hot separation using the Taguchi method

The signal-to-noise ratio (S/N) is used to analyze the data. Depending on the analysis, three cases may be of interest: lower is better, higher is better, or nominal is better. In this study, greater y-displacement is preferred, as it reduces the risk of stage collisions. The S/N ratio for this case is calculated using the following formula:

$$\frac{S}{N} = -10 \log_{10} \left[\frac{1}{n} \sum_{i=1}^n \frac{1}{y_i^2} \right] \quad (8)$$

Where n is the number of experiments and y_i is the measured output in each experiment.

After calculating the distances between the two stages for each experiment in Table 3, the S/N ratio values for each parameter are shown in Fig. 13. Increasing motor thrust, altitude, and flight Mach number increases the distance between the two stages, in agreement with earlier results. Based on the S/N ratio maximization and the levels defined in Table 4 and the results shown in Fig. 13, the optimal conditions for maximizing the distance between

the stages are a motor thrust of 420 kN, a Mach number of 2.9, an angle of attack of 1 degree, and a flight altitude of 16 km. Among the factors, the motor thrust exhibits the highest uncertainty, while the angle of attack has the slightest uncertainty.

6. CONCLUSION

This study investigated the hot separation process of a two-stage launch vehicle using a six degrees of freedom (6DOF) model in a three-dimensional simulation. The important parameters influencing this event, including altitude, flight Mach number, and angle of attack, were evaluated. The main findings can be summarized as follows:

Increasing altitude leads to more significant displacement of both stages along the flight path (y-axis) after hot separation, meaning that the two stages move further apart as altitude increases. Similarly, increasing the flight Mach number at the moment of separation results in

a more significant displacement of the first stage along the y-axis, while the second stage's displacement decreases. However, the distance between the two stages increases with higher Mach numbers. Additionally, increasing the angle of attack does not significantly affect the y-axis displacement. However, it increases the displacement of both stages in the x-axis (perpendicular to the flight path), causing the launch vehicle to deviate from its intended path. This makes controlling the second stage after separation more critical.

Finally, using the Taguchi method, it was concluded that motor thrust has the most significant impact on increasing the distance between the two stages and preventing collisions. In contrast, the angle of attack has a minor influence on this outcome.

This study focused on hot separation at low altitudes, where air density is high, and the Navier-Stokes equations govern flow dynamics. For future research, it is recommended to employ an aerodynamic model capable of accounting for rarefied gas conditions at higher altitudes. Additionally, the use of more advanced turbulence models could further enhance the accuracy of flow regime predictions during hot separation. Also it is recommended to numerically model the inter-stage adapter to evaluate its impact on separation parameters. Experimental studies could be conducted to evaluate the adapter's potential impact on second-stage motor choking rates during ignition

CONFLICT OF INTEREST

The author declares that there is no conflict of financial or non-financial interest to disclose.

AUTHORS CONTRIBUTION

D. Nasiri: Data curation, Investigation, Software, Visualization, Formal analysis, Writing – original draft; **M. Adami:** Data curation, Methodology, Visualization, Supervision, Writing – review & editing; **H. Taei:** Investigation, Visualization, review & editing; **H. Parhizkar:** Investigation, Software, Visualization, Formal analysis, Methodology, Writing – review & editing.

REFERENCES

- Bird, G. A. (1978). Monte Carlo Simulation of gas flows. *Annual Review of Fluid Mechanics*, 10, 11–31. <https://doi.org/10.1146/annurev.fl.10.010178.000303>
- Bird, G. A. (1981). Monte-carlo simulation in an engineering context. *Progress in Astronautics and Aeronautics*, 74, 239–55. <https://doi.org/10.2514/5.9781600865480.0239.0255>
- Collins, F. G., & Knox, E. C. (1994). Determination of wall boundary conditions for high-speed-ratio direct simulation monte carlo calculations. *Journal of Spacecraft and Rockets*, 31(6), 965–70. <https://doi.org/10.2514/3.26545>.
- Goldman, R. L. (1969). *Saging Loads*. NASA SP-8022.
- Huitong, L., Yang, Z., & Yixin, H. (2015, July). *Missile stage separation simulation considering complex factors*. 2015 34th Chinese Control Conference (CCC) (pp. 8768-8772). IEEE.
- Huseman, P. (1995). *CFD analysis of Titan IV fire-in-the-hole staging*. 33rd Aerospace Sciences Meeting and Exhibit (p. 352). American Institute of Aeronautics and Astronautics.
- Kumar, P., Swaminathan, R., Unnikrishnan, C., Ashok, V., & Adimurthy, V. (1998, July). Modelling of jet impingement forces during hot stage-separation of a launch vehicle. *34th AIAA/ASME/SAE/ASEE Joint Propulsion Conference and Exhibit* (p. 3156). Joint Propulsion Conferences. American Institute of Aeronautics and Astronautics.
- Lawson, S. J., & Barakos, G. N. (2011). Review of numerical simulations for high-speed, turbulent cavity flows. *Progress in Aerospace Sciences* 47(3), 186–216. <https://doi.org/10.1016/j.paerosci.2010.11.002>.
- Li, Y., Reimann, B., & Eggers, T. (2014). Numerical investigations on the aerodynamics of SHEFEX-III launcher. *Acta Astronautica*, 97, 99-108. <http://dx.doi.org/10.1016/j.actaastro.2014.01.006>
- Li, Y., Reimann, B., & Eggers, T. (2016). Coupled simulation of CFD-flight-mechanics with a two-species-gas-model for the hot rocket staging. *Acta Astronautica*, 128, 44-61. <https://doi.org/10.1016/j.actaastro.2016.07.009>.
- Martins Neto, F. (2020). Concepção de um veículo lançador de microssatélite baseado em foguetes de sondagem desenvolvidos no Brasil.
- Matsuo, H., & Kawaguchi, J. I. (1995). MV launch vehicle. *Acta Astronautica*, 35, 597-603. [http://dx.doi.org/https://doi.org/10.1016/0094-5765\(94\)00227-D](http://dx.doi.org/https://doi.org/10.1016/0094-5765(94)00227-D).
- Mitikov, Y., & Shynkarenko, O. (2023). A new look at the hot separation of liquid rocket stages. *CEAS Space Journal*, 15(2), 319-328. <http://dx.doi.org/10.1007/s12567-021-00407-y>.
- Oran, E. S., Oh, C. K., & Cybyk, B. Z. (1998). Direct simulation Monte Carlo: recent advances and applications. *Annual Review of Fluid Mechanics*, 30(1), 403-441. <https://doi.org/10.1146/annurev.fluid.30.1.403>.
- Rao, B. N., Jeyakumar, D., Biswas, K. K., Swaminathan, S., & Janardhana, E. (2006). Rigid body separation dynamics for space launch vehicles. *The Aeronautical Journal*, 110(1107), 289-302. <https://doi.org/10.1017/S0001924000013166>
- Roshanian, J., & Talebi, M. (2008). monte carlo simulation of stage separation dynamics of a multistage launch vehicle. *Applied Mathematics and Mechanics*, 29(11), 1411–26. <https://doi.org/10.1007/s10483-008-1103-z>.
- Simplicio, P. V., & Bennani, S. (2015, April). *Worst-case launch vehicle stage separation analysis*. In 3rd

CEAS Specialist Conference on Guidance, Navigation and Control, Toulouse, France.

- Singaravelu, J., Jeyakumar, D., & Rao, B. N. (2009). Taguchi's approach for reliability and safety assessments in the stage separation process of a multistage launch vehicle. *Reliability Engineering & System Safety*, 94(10), 1526-1541. <https://doi.org/10.1016/j.res.2009.02.017>.
- Wang, J. (1997). *Coupled CFD and rigid body dynamics analysis for the launch vehicle stage separation*. 33rd Joint Propulsion Conference and Exhibit, Joint Propulsion Conferences. American Institute of Aeronautics and Astronautics.
- Wang, Z. J., Yi-Zhao, W. U., & Jing-Zhou, L. I. N. (2009). Wind tunnel test on effect of the jet flow interaction on stage separation of launch vehicle. *Journal of Experiments in Fluid Mechanics*, 23(2), 15–19. <https://doi.org/10.3969/j.issn.1672-9897.2009.02.004>.
- Wasko, R. A. (1961). Experimental investigation of stage separation aerodynamics.